# Modelling of Slag Thermodynamic Properties. From Oxides to Oxisulphides.

H. Gaye and J. Lehmann

IRSID, Maizières - lès - Metz, France.

## ABSTRACT

After a brief survey of slag thermodynamic models, and their contribution to the understanding of metal-slag-inclusions-refractories reactions in Iron- and Steelmaking, the recent developments of IRSID slag model are presented. A new extension concerns the description of liquid oxisulphides, which is of great interest for the control of inclusions in some semi-killed steel grades. For these systems, a new expression of the configurational entropy was derived to describe short range order around the anions. It takes into account not only the nearest cations, but also the nearest anion neighbors. The new formalism can be applied to pure liquid oxide or sulphide systems, as well as to liquid oxisulphides. Its application to the description of phase diagrams in the system $SiO_2$ - MnO - MnS - FeO - FeS is presented and the estimation of sulphide capacities in multicomponent systems is compared to the results of the previous model.

## 1. INTRODUCTION

The traditional role of slag in Iron- and Steelmaking processes is to eliminate the gangue of the charged materials, and to refine the metal, as major contaminants of the steel can only be removed via the slag phase (S, P, ...). Another function has more recently been fully exploited, in the constant drive for higher purity and better and better controlled steel products: the fine adjustment of steel composition by slag treatment in ladle metallurgy in order to promote an adequate inclusionnary state.

In recent years, the optimization of high temperature metal-slag-refractories reactions in order to improve metal purity, and the control of the precipitation of endogeneous oxide and sulphide inclusions in steels have significantly progressed through the use of thermodynamic models of oxide systems[1]. The type of thermodynamic information needed concerns slag phase diagrams (definition of liquid domains for adequate operation of the reactors, crystallization behaviour of oxide inclusions) and component activities (or related quantities, for instance slag-metal equilibrium partition ratios, sulphide capacity, ...).

To represent industrial processes, thermodynamic models must describe multicomponent systems, as the metal quality will very often be conditioned by minor components of the slag. They should also be reasonably time efficient since the values of slag properties have to be reactualized a large number of times during the calculation, when used in kinetic reaction models or in multiphase equilibrium codes.

After a brief survey of slag thermodynamic models which have been proposed in the last few years, a recent development of IRSID slag model for the description of liquid oxisulphides is presented. The principles of this new formalism are outlined, and the results obtained for the description of the phase diagrams of the $SiO_2$-MnO-MnS and FeO-FeS-MnO-MnS systems, and for the description of sulphide capacities in the system $SiO_2$-$Al_2O_3$-MnO-MgO-CaO are compared to experimental results.

## 2. SLAG MODELLING APPROACHES

The main slag systems of interest in Iron- and Steelmaking are summarized in Figure 1., showing the diversity of components and composition ranges. In this diagram, the main components have been grouped as acid components ($SiO_2$ ...), basic components (CaO ...) and fluxing agents ($Al_2O_3$, FeO ...).

Until the development of statistical thermodynamics models, one had to rely on rather crude correlations of slag thermodynamic properties as a function of temperature and composition. Among the most successful

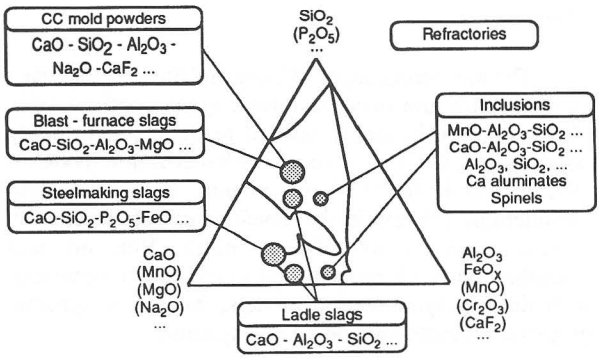


Fig. 1. Main classes of iron- and steelmaking slags and inclusions.

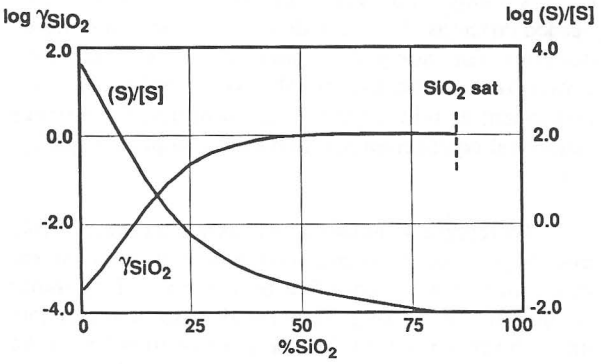


Fig. 2. Variation of $SiO_2$ activity coefficient and S partition coefficient at equilibrium with liquid steel containing 0.3 %Si, in the pseudo-binary system 60%CaO-40%$Al_2O_3$ / $SiO_2$ at 1600°C.

of these early methods, we may mention Flood-Grjotheim's model[2] and adaptations[3] whose domain of application, although very important industrially, is limited to extremely basic refining slags. Correlations of thermodynamic properties (for instance, sulphide capacity) in terms of "optical basicity index" were also proposed[4]. Although they can be useful for limited composition ranges in some specific systems, their extrapolation over domains in which they have not been fitted can lead to considerable errors[5] (typically several orders of magnitude in slags containing Mn and Fe oxides). Indeed, as illustrated in Figure 2, the slag properties may change drastically over very limited composition ranges, when going from the domain of basic slags (CaO rich slags) to that of acid slags ($SiO_2$ rich slags). In the pseudo binary system considered in this figure, the activity coefficient of $SiO_2$ increases sharply in the 0 to 25 %$SiO_2$ domain and keeps a value around 1 at higher silica contents, whereas the sulphur equilibrium partition coefficient decreases from about 3000 to 1 in the basic domain and is well below unity in the acid domain. These sharp variations of thermodynamic properties also explain that regular solution models or other polynomial representations in terms of contents in oxide components, even though they can provide accurate fitting of activities in some restricted domains[6-7], should be used cautiously in other domains, as extrapolations may lead to substantial errors.

The pioneering paper of Toop and Samis[8], focussing on an equilibrium between three oxygen configurations (free oxygen $O^{2-}$, singly bonded to Si, $O^-$, and doubly bonded to Si, $O^o$) and Masson's polymerization model of silicate tetrahedra[9-11] have, in their time, stimulated considerable interest in the development of structurally oriented models of silicate melts. Yet, no real breakthrough has been achieved to this day to represent, with these polymerization models, the thermodynamic properties of multicomponent slag systems.

A novel approach using a concept of oxygen and cation sublattices was introduced in the early 1970's by Yokokawa and Niwa[12] and Kapoor and Frohberg[13], with, however, no applications beyond a few ternary systems. This approach was then generalized at IRSID to represent the properties (component activities and phase diagrams) of systems containing large numbers of oxide components[14], and was later on extended to systems containing, in addition, fluor and sulphur at diluted contents[15]. A similar approach using an adaptation of the quasichemical theory has been developed by Blander and Pelton first for binary silicates[16], and later on for ternary silicates[17].

In IRSID's model for pure oxides, the liquid slag is represented using an oxygen sublattice and a cationic sublattice filled with the different cations in decreasing order of their charge. The structure is then described in terms of cells composed of a central oxygen surrounded by two cations. Two types of parameters are used to evaluate the energy of the system : the energies for the formation of asymmetric cells from the corresponding symmetrical cells, and interaction energies limited to one parameter per couple of cations. Thus, only a limited number of binary parameters (two per binary system) are used to describe multicomponent systems, and for the systems investigated so far, they have been assumed to be temperature independent. It may however be necessary to assess them in systems containing more than two components, as binary data is frequently lacking or not accurate enough, in particular because the liquid domain of binary systems of interest is often too narrow in the relevant domain of temperature. In order to fit the model parameters on multicomponent data, a computer code based on a least squares approximation technique has been written. It can handle various types of thermodynamic information:

- slag component activities,
- various quantities directly derived from the slag component activities (slag/metal equilibrium partition ratios, ...),
- information on phase diagrams. Data on phase diagrams can be expressed as chemical potentials of stoichiometric compounds, but also in terms of position of liquidus line. In this case, the regression is no longer based on chemical potential data, but on composition variables data.

To the liquid phase model are associated the values of energy of formation of the various stoichiometric compounds that can be formed at lower temperature, as well as solution models for various solid solutions (spinels, olivine, ...). Some of these values have been adapted in order to obtain a best fit of the phase diagrams, while remaining within the range of uncertainty of the experimentally determined thermochemical data.

At present, the model has been validated, and is used in our steel plants and laboratories in the multiphase equilibrium calculation code CEQCSI[1], for the system $SiO_2$-$TiO_2$-$Ti_2O_3$-$Cr_2O_3$-$Al_2O_3$-$Fe_2O_3$-CrO-FeO-MgO-MnO-CaO with in addition up to 10-20 %$CaF_2$ and a few percents of sulphur.

## 3. MODELLING OF OXISULPHIDE SYSTEMS

In our earliest evaluations of equilibrium sulphur partition between steel and ladle slag[18-19], sulphide capacity correlations[4] were combined with an evaluation, using the slag model, of the oxygen potential at equilibrium between appropriate deoxidizors dissolved in the metal and their oxides in the slag. This method gave acceptable results for highly basic slags limited to the system $SiO_2$-$Al_2O_3$-CaO-MgO, but the evaluation of sulphur content was in error by several orders of magnitude for slags containing, in addition, large amounts of manganese and iron oxides. This discrepancy is due to an inadequacy of the sulphide capacity / optical basicity correlation for these slags.

In a second stage[15], the slag model was altered to introduce limited amounts of anionic species other than O (that is S and F). The corresponding model parameters have been assessed at this time for the whole system indicated above, and they provide accurate estimations of equilibrium sulphur partition coefficients. However, this version of the model, which will be referred to in the following as the "intermediate model", cannot be extrapolated to oxisulphide systems containing large amounts of sulphur, which can be encountered as inclusions in certain grades of resulphurized semi-killed steels. To fill this gap, the model has been modified to take better account of the anionic surroundings on the anion sublattice.

### 3.1 Description of the oxisulphide model

The formalism used in the oxisulphide model can be applied to an arbitrary number of anions and cations, and is based on the same general assumptions as in the intermediate model :

- two sublattices are considered, an anionic sublattice occupied by the anions, assumed divalent, and a cationic sublattice, filled with the various cations ranked in the decreasing order of their valencies,

- the structure is then described in terms of cells. In the previous model, a cell described only the cationic neighborhood of the various anions. Thus, the cell i-k-j consisted of the central anion k, and two peripheral cations i and j, and the number of these cells was noted $R_{ij}^{k}$. In the new model, the structural entity consists of a central anion with two adjacent cations and a shell of Z anion nearest neighbors. In the applications made so far, we have arbitrarily set Z=6. Thus, a cell with central ion k, cationic neighbors i and j, and anionic shell containing $n_1$ anions "1", ... $n_p$ anions "p", is noted $\underset{i,\,j}{\overset{n_1,\,\ldots\,n_p}{k}}$, and the number of these cells is noted $R_{ij}^{k\ n_1,\,\ldots\,n_p}$.

The partition function of the solution is described in terms of the probabilities associated with the different configurations of these cells. The summation is extended to all the anions, each one being considered in turn as a central anion. The various definitions, system of equations to be solved to maximize the partition function, and expression of the Gibbs free energy of the system are listed in the Appendix A. The calculation requires, for one temperature and composition in a system containing m cations and p anions, the resolution of a system of m + 2(p-1) non linear equations. In comparison with the previous model, there is one additional equation per anion.

The energy parameters of the model are energies of cells formation and of interactions between cells.

Parameters of cells formation:

- $W_{ij}^{kq}$ is associated to the formation of asymmetric cells from symmetric ones, in which the central anion is k and all the anions in the nearest neighbor shell are identical and noted q, according to the reaction:

$$\frac{1}{2}\cdot\underset{i,\,i}{\overset{n_q=Z}{k}} + \frac{1}{2}\cdot\underset{i,\,j}{\overset{n_q=Z}{k}} = \underset{i,\,j}{\overset{n_q=Z}{k}}$$

All these parameters have so far been considered to be temperature independent. A few of them vary linearly with composition in the binary systems.

- $W_{ii}^{Ok}$ is associated to the replacement of Z anions O by Z anions k in the nearest neighbor shell of a symmetric cell, according to the reaction:

$$\underset{i,\,i}{\overset{n_O=Z}{O}} + k = \underset{i,\,i}{\overset{n_k=Z}{O}} + O$$

This parameter is assumed to be equal to the parameter $W_{ii}^{kO}$ associated to the exchange between O and k as the central anion of cells in which all anions in the nearest neighbor shell are O. Indeed, in both cases, the reaction corresponds to the replacement of Z O-O bonds by Z k-k bonds. Similarly, it is assumed that if only one O in the nearest neighbor shell is replaced by one k, the corresponding parameter is $1/Z\ W_{ii}^{Ok}$.

- $W_{ii}^{kq}$ is associated to the replacement of O by k as central anion, and the replacement of Z anions O by Z anions q in the nearest neighbor shell of a symmetric cell, according to the reaction:

$$\underset{i,\,i}{\overset{n_O=Z}{O}} + k + q = \underset{i,\,i}{\overset{n_q=Z}{k}} + 2O$$

When q=k (for instance, representing S), this parameter corresponds to the $\Delta G°$ associated with the formation of the pure sulphide from the pure oxide, with elements S and O dissolved in liquid iron:

$$\frac{1}{v_i}(M_i)_{u_i}(O)_{v_i} + \underline{k} = \frac{1}{v_i}(M_i)_{u_i}(k)_{v_i} + \underline{Q}$$

These last parameters vary with temperature and have been selected according to the thermochemical values.

Parameters of interactions between cells:

The parameters of interactions between cells have been kept identical to the ones in the previous model, assuming the effect of the cationic shell is negligible. Two types of parameters are thus used:

- $E_{ij}^{kk}$, which describes the interaction between a cell $\underset{i,\,i}{\overset{n_1,\ldots n_p}{k}}$ and a cell $\underset{i,\,j}{\overset{n_1',\ldots n_p'}{k}}$, i being a cation with a valency larger than that of j.

- $E_{ii}^{kq}$, describing the interaction between two symmetric cells, $\underset{i,\,i}{\overset{n_1,\ldots n_p}{k}}$ and $\underset{i,\,j}{\overset{n_1',\ldots n_p'}{q}}$.

The total number of parameters , for a system composed of m cations and p anions, is equal to mp.(m+1).(p+3)/4 - 2m. Thus, for the system Si-Mn-O-S, up to 11 parameters can be used: $W_{SiMn}^{OO}$, $W_{SiMn}^{OS}$, $W_{SiMn}^{SS}$, $W_{SiSi}^{OS}$, $W_{MnMn}^{OS}$, $W_{SiSi}^{SS}$, $W_{MnMn}^{SS}$, $E_{SiMn}^{OO}$, $E_{SiMn}^{SS}$, $E_{SiSi}^{OS}$ and $E_{MnMn}^{OS}$, that is 3 additional parameters with respect to the intermediate model.

In the various systems which have been studied, all the oxide model parameters have kept the values which had been determined for the intermediate model[15], and only some of the sulphide parameters and of the additional ones have been assessed from information on the oxisulphide systems.

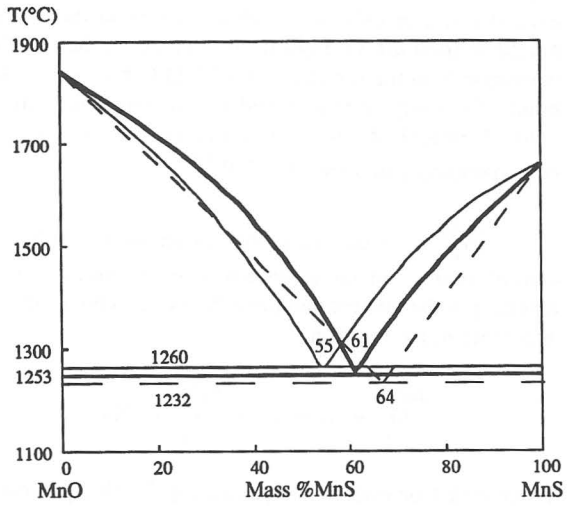


Fig. 3. Comparison of the calculated MnO-MnS phase diagram (thick line) with the experimental diagram proposed by Fisher[20] (thin line) and Chao[21] (dotted line).

3.2 The $SiO_2$ - MnO - MnS system

The model parameters have been adjusted in order to obtain a best fit of the phase diagram from experimental data on the binary MnO-MnS[20-21], and on the ternary $SiO_2$-MnO-MnS[22-23]. The values of the new parameters are listed in Table I.

Table I. Values of the new parameters (cal.mol$^{-1}$) used, in addition to the parameters given in Ref 15, to describe the $SiO_2$ - MnO - MnS system

| | $W_{ij}^{OS}$ | $W_{ij}^{SS}$ |
|---|---|---|
| Si-Si | 44230-10T | 76013-12.74T |
| Si-Mn | 3200 | 28000 |
| Mn-Mn | 7900-1.48T | 27100-8.05T |

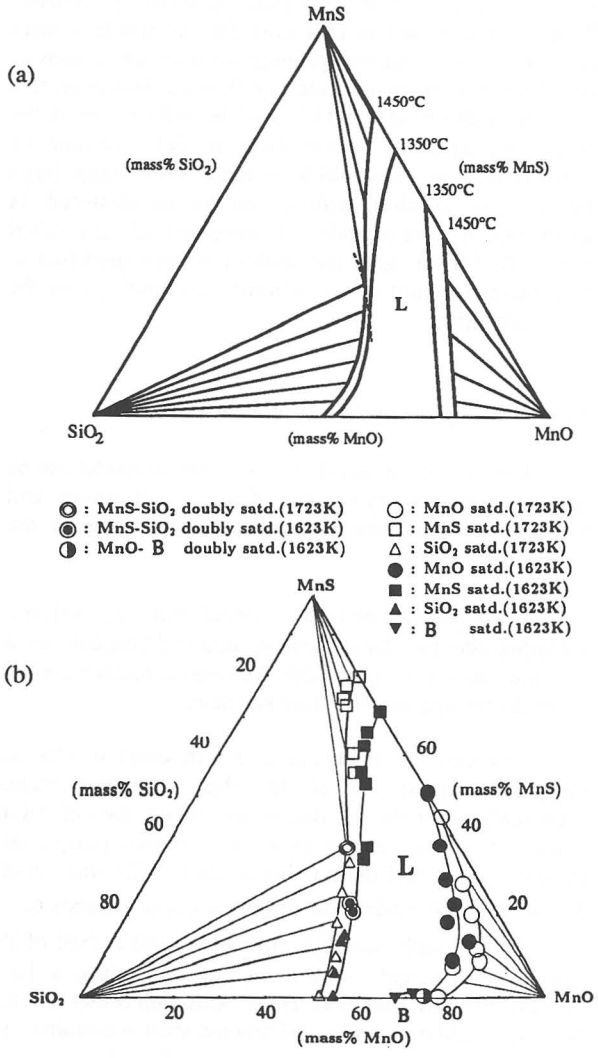


Fig. 4. Comparison of the calculated $SiO_2$-MnO-MnS phase diagram (a) with the experimental diagram determined by Hasegawa et al.[23] (b).

As shown in Fig 3 and 4, the calculated diagrams are in satisfactory agreement with the experimental determinations. In the binary MnO-MnS systems, the position of the eutectic point in the two experimental determinations is quite different (55 %MnS - 1260°C, and 64 %MnS - 1232°C, respectively). We have arbitrarily assessed the parameters in order to obtain an intermediate position: 61 %MnS and 1253°C. In the ternary system, the very high MnS solubilities are quite well described by the model.

### 3.3 The FeO - FeS - MnO - MnS system in equilibrium with Fe.

This system contains in fact 3 cations, $Fe^{2+}$, $Fe^{3+}$ and $Mn^{2+}$ and two anions, $O^{2-}$ and $S^{2-}$. The model parameters have been assessed from experimental information of the phase diagrams of the FeO-FeS[24] and FeO-FeS-MnO-MnS[25-26] systems in equilibrium with Fe.

Table II. Values of the new parameters (cal.mol$^{-1}$) used, in addition to the parameters given in Ref 15, to describe the FeO - FeS - MnO - MnS system.

| | $W_{ij}^{OS}$ | $W_{ij}^{SS}$ |
|---|---|---|
| $Fe^{3+}$-$Fe^{3+}$ | 30000 | 30000 |
| $Fe^{3+}$-$Fe^{2+}$ | 0 | 0 |
| $Fe^{3+}$-Mn | 0 | 0 |
| $Fe^{2+}$-$Fe^{2+}$ | 30248-16.27T | 26423-7.09T |
| $Fe^{2+}$-Mn | 8000 | 8000 |
| Mn-Mn | 7900-1.48T | 27100-8.05T |

As shown in Fig. 5 and 6 there is a fair agreement between calculated and experimental diagrams. Note, in particular, that the slight discrepancy on the MnO-MnS side of the quaternary system with the diagram compiled by Oelsen and Schürmann comes from the choice, by these last authors, of a binary diagram different from the ones generally accepted[20-23,26].

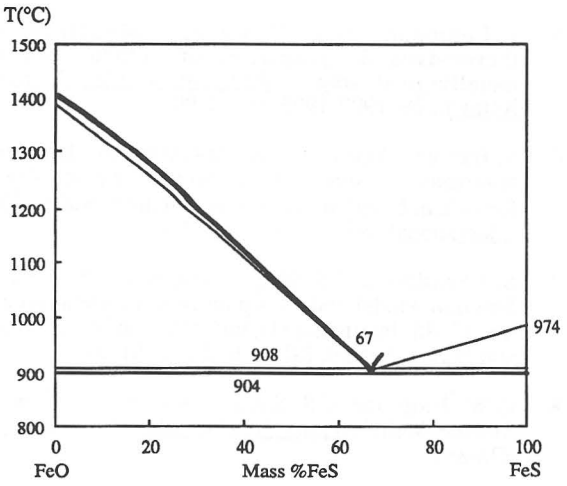


Fig. 5. Comparison of the calculated FeO-FeS phase diagram at equilibrium with iron (thick line) with the experimental diagram[24] (thin line).

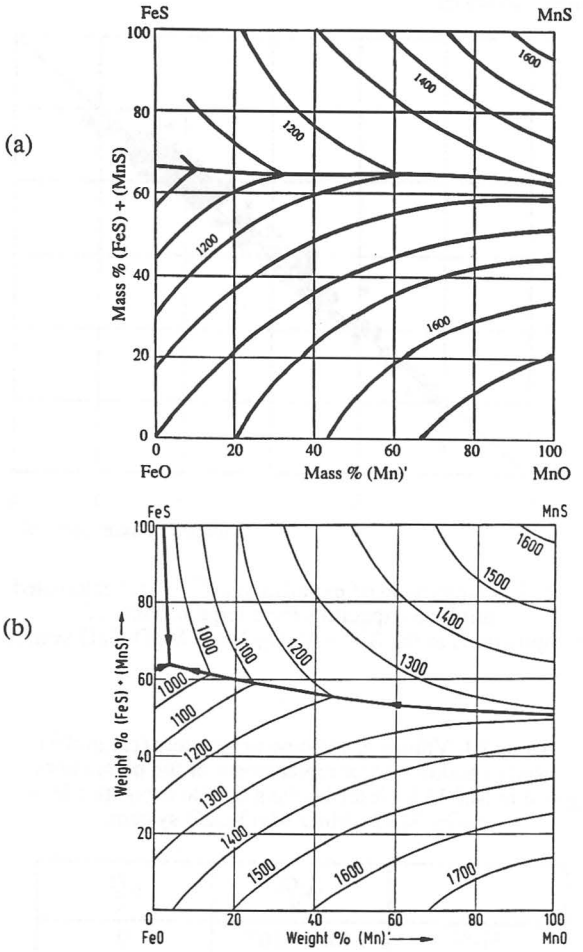


Fig. 6. Comparison of the calculated FeO-FeS-MnO-MnS phase diagram (a) with the experimental diagram compiled by Oelsen and Schürmann[25] (b).

### 3.4 Description of the sulphide capacities in the $SiO_2$-$Al_2O_3$-MnO-MgO-CaO system.

Due to the modifications in the model formalism, it was necessary to reassess some of the model parameters which had been determined in the intermediate model[15]. The new values, for the $SiO_2$-$Al_2O_3$-MnO-MgO-CaO system have been obtained from a large quantity of experimental data[27-37]. They are listed in Table III.

As shown in Fig. 7, which compares the calculated and experimental values for a large number of slag compositions in this system, the precision on the evaluation of the sulphide capacity is quite good, about identical as for the intermediate model.

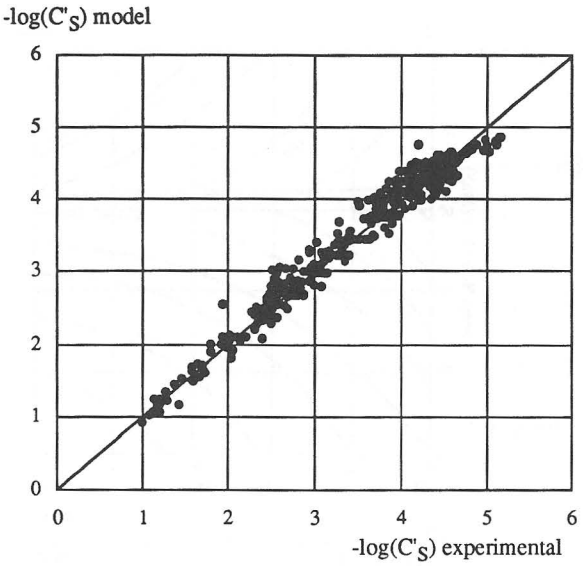


Fig. 7. Comparison of experimental[27-37] and calculated sulphide capacities for a large number of compositions in the $SiO_2$-$Al_2O_3$-MnO-MgO-CaO system.

Table III. Values of the new parameters (cal.mol$^{-1}$) used in addition to or replacement of the parameters given in Ref 15 to describe the sulphide capacities in the $SiO_2$-$Al_2O_3$-MnO-MgO-CaO system.

| | $W_{ij}^{OS}$ | $E_{ij}^{SS}$ |
|---|---|---|
| Si-Si | 44230-10T | 0 |
| Si-Mn | 3200 | 0 |
| Si-Mg | 8500 | 0 |
| Si-Ca | 2290 | 0 |
| Al-Al | 36500 | -760 |
| Al-Mn | 4090 | 0 |
| Al-Mg | 6760 | 0 |
| Al-Ca | 9480 | 0 |
| Mn-Mn | 7900-1.48T | 0 |
| Mn-Mg | -2900 | 0 |
| Mn-Ca | -1930 | 0 |
| Mg-Mg | 13300 | 0 |
| Mg-Ca | -2875 | 0 |
| Ca-Ca | -400 | 440 |

## 4. CONCLUSIONS

The exploitation of information on the thermodynamics properties of steelmaking slags has strongly progressed in the last few years, mainly through the use of various approaches of statistical thermodynamics models. It is now possible to describe the complex industrial systems accurately enough to use efficiently this information in the definition of treatments for improved metal purity and better control of the precipitation of endogeneous inclusions in steels.

The model developped at IRSID is consistenly expanded in two directions in order to enlarge its range of application:

- by increasing the number of oxide components which can be treated simultaneously. It is presently used for calculations in the system $SiO_2$-$TiO_2$-$Ti_2O_3$-$Cr_2O_3$-$Al_2O_3$-$Fe_2O_3$-CrO-FeO-MgO-MnO-CaO with additions of up to 10-20 %$CaF_2$ and a few %S,
- by increasing the replacement range of O by other anions (S, F). The last extension allows the description of the full range of oxisulphide compositions from pure oxides to pure sulphides. This change is made with minimal complication, that is by keeping most of the parameters determined in the previous version of the model, and adding only a few ones, all binary.

## REFERENCES


1. H. Gaye, C. Gatellier and P.V. Riboud, "Control of Endogeneous Inclusions in Al-killed and low-Al Steels", Proceedings of the Ethem T. Turkdogan Symposium, The Iron and Steel Society, (1994), pp. 113-124.
2. H. Flood and K. Grjotheim, "Thermodynamic Calculation of Slag Equilibria", J. Iron Steel Inst., 171, 1952, pp. 64-70.
3. H. Gaye, J.C. Grosjean and P.V. Riboud, "Estimation de l'équilibre métal-laitiers basiques d'aciérie. Application à l'étude des performances de réacteurs industriels", Congrès PCS 78, Société Française de Métallurgie, Versailles, (1978), pp. 244-245.
4. D.J. Sosinsky and I.D. Sommerville, "The Composition and Temperature Dependence of the Sulfide Capacity of Metallurgical Slags", Metall. Trans. B, vol. 17B, 1986, pp. 331-337.
5. J. Lehmann and H. Gaye, "Modeling of thermodynamic properties of sulphur bearing metallurgical slags", Rev. Int. Hautes Tempér. Réfract., 28, 1992-1993, pp. 81-90.
6. S. Ban-ya, "Mathematical expression of slag-metal reactions in steelmaking process by quadratic formalism based on the regular solution model", ISIJ International, vol. 33, 1993, pp. 2-11.
7. S. Jahanshahi and S. Wright, "Aspects of the Regular Solution Model and its Application to Metallurgical Slags", 4th International Conference on Molten Slags and Fluxes, Sendai, ISIJ, (1992), pp. 61-66.
8. G.W. Toop and C.S. Samis, "Activities of Ions in Silicate Melts", Trans. TMS-AIME, 224, 1962, pp. 878-887.
9. C.R. Masson, "An Approach of the Problem of Ionic Distribution in Liquid Silicates", Proc. Roy. Soc. (London), A287, 1965, pp. 201-221.

10. C.R. Masson, "Thermodynamics and Constitution of Silicate Slags", in Chemical Metallurgy of Iron and Steel, Iron and Steel Institute, London, (1973), pp. 3-11.

11. D.R. Gaskell, "Thermodynamic Models of Liquid Silicates", Can. Met. Quart., 20, 1981, pp. 3-19.

12. T. Yokokawa and K. Niwa, "Free Energy of Solution in Binary Silicate Melts", Trans. Jap. Inst. Metals, 10, 1969, pp. 3-7 and 81-86.

13. M.L. Kapoor and M.G. Frohberg, "Theoretical Treatment of Activities in Silicate Melts", in Chemical Metallurgy of Iron and Steel, Iron and Steel Institute, London, (1973), pp. 17-22.

14. H. Gaye and J. Welfringer, "Modelling of the Thermodynamic Properties of Complex Metallurgical Slags", Proc. Second International Symposium on Metallurgical Slags and Fluxes, Eds. H.A. Fine and D.R. Gaskell, Warrendale, PA, (1984), pp. 357-375.

15. H. Gaye, J. Lehmann, T. Matsumiya and W. Yamada, "A Statistical Thermodynamics Model of Slags: Applications to Systems containing S, F, $P_2O_5$ and Cr Oxides", 4th International Conference on Molten Slags and Fluxes, Sendai, ISIJ, (1992), pp. 103-108.

16. A.D. Pelton and M. Blander,"Computer-assisted analysis of the Thermodynamic Properties and Phase Diagrams of Slags", Proc. Second International Symposium on Metallurgical Slags and Fluxes, Eds. H.A. Fine and D.R. Gaskell, Warrendale, PA, (1984), pp. 281-294.

17. M. Blander, A. Pelton and G. Eriksson, "Analyses and Predictions of the Thermodynamic Properties and Phase Diagrams of Silicate Melts", 4th International Conference on Molten Slags and Fluxes, Sendai, ISIJ, (1992), pp. 56-60.

18. M. Faral and H. Gaye, "Metal - Slag Equilibria", Proc. Second International Symposium on Metallurgical Slags and Fluxes, Eds. H.A. Fine and D.R. Gaskell, Warrendale, PA, (1984), pp. 159-179.

19. H. Gaye et al., "Slags and inclusions control in secondary steelmaking", Clean Steel Conference, Balatonfüred, Hungary, June 1986.

20. W.A. Fisher and P.W. Bardenheuer, "Die Gleichgewichte zwischen mangan-, schwefel- und sauerstoff-haltigen Eisenschmelzen und ihren Schlacken im Mangan(II)-oxydtiegel bei 1530 bis 1800°C", Arch. Eisenhüttenwes., 41, 1970, pp. 119-124.

21. H.C. Chao, Y.E. Smith, and L.H. Van Vlack, "The MnO-MnS phase diagram", Trans. Met. Soc. AIME, 227, 1963, pp 796-797.

22. N. Koyama, F. Tsukihashi and N. Sano, "The solubilities of MnS in $MnO-SiO_2-TiO_2$ melts", Tetsu-to-Hagane, Vol. 79, 1993, pp 1334-1337.

23. A. Hasegawa, K. Morita and N. Sano, "Phase equilibria for the $MnO-SiO_2$-MnS slag system", Tetsu-to-Hagane, Vol. 81, 1995, pp 1109-1113.

24. E.T. Turkdogan and G.J.W. Kor with Appendix by L.S. Darken and R.W. Gurry, "Sulfides and Oxides in Fe-Mn alloys: Part I. Phase relations in Fe-Mn-S-O system", Metall. Trans., 2, 1971, pp. 1561-1570.

25. W. Oelsen, and E. Schürmann, Hütte - Taschenbuch für Eisenhüttenleute, Berlin/Düsseldorf, (1961) - Slag Atlas, 2nd Edition, Edited by VDEh, (1995), p. 208.

26. E.N. Silverman, "Synthetic inclusions in the FeO-MnO-MnS-$SiO_2$ system in equilibrium with resulfurized steel", Trans. Met. Soc. AIME, 221, 1961, pp. 512-517.

27. R.A. Sharma and F.D. Richardson, "Activities of manganese oxide, sulfide capacities and activity coefficients in aluminate and silicate melts", Trans. Met. Soc. AIME, 233, 1965, pp. 1586-1592.

28. R.A. Sharma and F.D. Richardson, "Activities in lime-alumina melts", J. Iron and Steel Inst., 198, 1961, pp. 386-390.

29. R.A. Sharma and F.D. Richardson, "The solubility of calcium sulphide and activities in lime-silica melts", J. Iron and Steel Inst., 200, 1962, pp. 373-379.

30. C.J.B. Fincham and F.D. Richardson, "Sulphur in silicate and aluminate slags", Proc. Roy. Soc. (London) , A 223, 1954, pp. 40-62.

31. K.P. Abraham, M.W. Davies and F.D. Richardson, "Sulphide capacities in silicate melts. Part I", J. Iron and Steel Inst., 196, 1960, pp. 309-312.

32. K.P. Abraham and F.D. Richardson, "Sulphide capacities in silicate melts. Part II", J. Iron and Steel Inst., 196, 1960, pp. 313-317.

33. M.R. Kalyanram, T.G. MacFarlane and H.B. Bell, "The activity of calcium oxide in slags in the systems $CaO-MgO-SiO_2$, $CaO-Al_2O_3-SiO_2$ and $CaO-MgO-Al_2O_3-SiO_2$ at 1500°C", J. Iron and Steel Inst., 195, 1960, pp. 58-64.

34. G.J.W. Kor and F.D. Richardson, "Sulphur in lime-alumina mixtures", J. Iron and Steel Inst., 206, 1968, pp. 700-704.

35. P.T. Carter, T.G. MacFarlane, "Thermodynamics of slag systems", J. Iron and Steel Inst., 185, 1957, pp. 54-66.

36. B. Ozturk and E.T. Turkdogan, "Equilibrium sulphur distribution between molten calcium aluminate and steel", Met. Sci., 18, 1984, pp. 299-309.

37. M. Hino, S. Kitagawa ans S. Ban-ya, "Sulphide capacities of $CaO-Al_2O_3-MgO$ and $CaO-Al_2O_3-SiO_2$ slags", Tetsu-to-Hagane, vol. 79, 1993, pp. 34-40.

## APPENDIX A: CALCULATION OF THE GIBBS FREE ENERGY.

### A1. Notations.

m number of cations.
p number of anions.
$u_i$, $v_i$ stoichiometric coefficients of $(M_i)_{u_i}(A_k)_{v_i}$ and $a_i=u_i/v_i$

$X_i^k$ mole numbers of $(M_i)_{u_i}(A_k)_{v_i}$

$V_i=\sum_{k=1}^{p} v_i.X_i^k \quad V^k=\sum_{i=1}^{m} v_i.X_i^k \quad D_i=\sum_{j=i}^{m} V_j$ (D stands for $D_1$).

$R_{ij}^{k\ n_1,\ldots,n_p}$ mole number of cells having i and j for nearest cation neighbors, and $n_1$ anions "1", $n_2$ anions "2",..., $n_p$ anions "p" for nearest anion neighbors.

$Z=\sum_{q=1}^{p} n_q$ number of nearest anion neighbors of a given anion.

$$RT\ln Q_i^k=\frac{1}{D}\left(\sum_{j=1}^{m} V_j.E_{ij}^k+\sum_{q=1}^{p} V^q.E_i^{kq}\right)$$

$$r_{ij}^{kq}=\exp\left(\frac{1}{z}.\left(W_{11}^{Oq}-\left(W_{ij}^{kq}-W_{ij}^{kO}\right)\right)\Big/RT\right)$$

$$p_{ij}^k=\exp\left(\left(-\frac{1}{2}.(1-\delta_{ij}).\left(W_{ii}^{kO}+W_{jj}^{kO}\right)+W_{11}^{kO}-W_{ij}^{kO}\right)\Big/RT\right).\frac{Q_i^O.Q_j^O}{(Q_i^k)^{2\delta_{ij}}}.\left(\frac{Q_1^k}{Q_1^O}\right)^2$$

### A2. Expression of the Gibbs free energy.

$$G=\sum_{i,j=1}^{m}\sum_{k=1}^{p}\sum_{n_2,\ldots,n_p=0}^{Z}\frac{Z!}{\prod_{q=1}^{p} n_q!}.\left(\sum_{q=1}^{p} n_q.W_{ij}^{kq}\right).R_{ij}^{k\ n_1,\ldots,n_p}+2\sum_{i=1}^{m}\sum_{k=1}^{p} RT\ln Q_i^k\sum_{n_2,\ldots,n_p=0}^{Z}\frac{Z!}{\prod_{q=1}^{p} n_q!}.R_{ii}^{k\ n_1,\ldots,n_p}$$

$$-RT\left[\sum_{i=1}^{m-1} a_i.\left(D_i.\ln\left(\frac{D_i}{V_i}\right)-D_{i+1}.\ln\left(\frac{D_{i+1}}{V_i}\right)\right)+2\sum_{i=1}^{m} V_i.\ln\left(\frac{V_i}{D}\right)+Z\sum_{k=1}^{p} V^k.\ln\left(\frac{V^k}{D}\right)\right]$$

$$+RT\sum_{i,j=1}^{m}\sum_{k=1}^{p}\sum_{n_2,\ldots,n_p=0}^{Z}\frac{Z!}{\prod_{q=1}^{p} n_q!}.R_{ij}^{k\ n_1,\ldots,n_p}.\ln\left(\frac{R_{ij}^{k\ n_1,\ldots,n_p}}{D}\right)$$

### A3. Maximisation of the partition function.

In the expression of the Gibbs free energy, the $R_{ij}^{k\ n_1,\ldots,n_p}$ are calculated by solving the following set of equations which are an expression of the condition of maximisation of the partition function, in terms of the unknowns $y_i$,$y^k$,$z^q$:

$$y_i.\sum_{j=1}^{m}\sum_{k=1}^{p} p_{ij}^k.y_j.y^k.\left(\sum_{q=1}^{p} r_{ij}^{kq}.z^q\right)^Z=V_i \qquad (i=1\ldots m)$$

$$y^k.\sum_{i=1}^{m}\sum_{j=1}^{m} p_{ij}^k.y_i.y_j.\left(\sum_{q=1}^{p} r_{ij}^{kq}.z^q\right)^Z=V^k \qquad (k=2\ldots p)$$

$$z^q.\sum_{i,j=1}^{m}\sum_{k=1}^{p} p_{ij}^k.y_i.y_j.y^k.r_{ij}^{kq}.\left(\sum_{l=1}^{p} r_{ij}^{kl}.z^l\right)^{Z-1}=V^q \qquad (q=2\ldots p)$$

Once the variables $y_i$,$y^k$,$z^q$ have been calculated, the mole numbers of cells are obtained according to:

$$R_{ij}^{k\ n_1,\ldots,n_p}=p_{ij}^k.y_i.y_j.y^k.\prod_{q=1}^{p}\left(r_{ij}^{kq}.z^q\right)^{n_q}$$